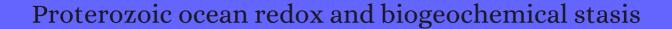
CITATION REPORT List of articles citing



DOI: 10.1073/pnas.1208622110 Proceedings of the National Academy of Sciences of the United States of America, 2013, 110, 5357-62.

Source: https://exaly.com/paper-pdf/55397061/citation-report.pdf

Version: 2024-04-28

This report has been generated based on the citations recorded by exaly.com for the above article. For the latest version of this publication list, visit the link given above.

The third column is the impact factor (IF) of the journal, and the fourth column is the number of citations of the article.

#	Paper	IF	Citations
373	Geochemistry of pyrite from diamictites of the Boolgeeda Iron Formation, Western Australia with implications for the GOE and Paleoproterozoic ice ages. <i>Chemical Geology</i> , 2013 , 362, 131-142	4.2	17
372	Uranium in iron formations and the rise of atmospheric oxygen. Chemical Geology, 2013, 362, 82-90	4.2	74
371	Coupled molybdenum, iron and uranium stable isotopes as oceanic paleoredox proxies during the Paleoproterozoic Shunga Event. <i>Chemical Geology</i> , 2013 , 362, 193-210	4.2	101
370	Molybdenum geochemistry in a seasonally dysoxic Mo-limited lacustrine ecosystem. <i>Geochimica Et Cosmochimica Acta</i> , 2013 , 114, 204-219	5.5	23
369	Geochemistry articles [April 2013. <i>Organic Geochemistry</i> , 2013 , 60, e1-e29	3.1	
368	Sulfur isotopes track the global extent and dynamics of euxinia during Cretaceous Oceanic Anoxic Event 2. <i>Proceedings of the National Academy of Sciences of the United States of America</i> , 2013 , 110, 184	10 7 -152	105
367	Scientific drilling and the evolution of the earth system: climate, biota, biogeochemistry and extreme systems. 2013 , 16, 63-72		5
366	Tackling the 99%: Can We Begin to Understand the Paleoecology of the Small and Soft-Bodied Animal Majority?. 2013 , 19, 77-86		8
365	Nitrogen isotope fractionation by alternative nitrogenases and past ocean anoxia. <i>Proceedings of the National Academy of Sciences of the United States of America</i> , 2014 , 111, 4782-7	11.5	100
364	Shallow stratification prevailed for ~1700 to ~1300 Ma ocean: Evidence from organic carbon isotopes in the North China Craton. <i>Earth and Planetary Science Letters</i> , 2014 , 400, 219-232	5.3	49
363	The Geologic History of Seawater. 2014 , 569-622		22
362	Sunspot cycles recorded in Mesoproterozoic carbonate biolaminites. <i>Precambrian Research</i> , 2014 , 248, 1-16	3.9	17
361	Fluctuation of shelf basin redox conditions in the early Ediacaran: Evidence from Lantian Formation black shales in South China. <i>Precambrian Research</i> , 2014 , 245, 1-12	3.9	32
360	Cobalt and marine redox evolution. Earth and Planetary Science Letters, 2014, 390, 253-263	5.3	72
359	The rise of oxygen in Earth's early ocean and atmosphere. 2014 , 506, 307-15		1355
358	Co-evolution of eukaryotes and ocean oxygenation in the Neoproterozoic era. 2014 , 7, 257-265		245
357	A neoproterozoic transition in the marine nitrogen cycle. 2014 , 24, 652-7		87

356	Nutrition: rejection is the fly's protection. 2014 , 24, R278-80		1
355	Geochemical, metagenomic and metaproteomic insights into trace metal utilization by methane-oxidizing microbial consortia in sulphidic marine sediments. 2014 , 16, 1592-611		35
354	Trace element content of sedimentary pyrite as a new proxy for deep-time ocean to mosphere evolution. <i>Earth and Planetary Science Letters</i> , 2014 , 389, 209-220	5.3	280
353	Chemical biology. A bump-and-hole approach to engineer controlled selectivity of BET bromodomain chemical probes. 2014 , 346, 638-641		108
352	Earth history. Low mid-Proterozoic atmospheric oxygen levels and the delayed rise of animals. 2014 , 346, 635-8		456
351	Nitrogen and sulfur assimilation in plants and algae. 2014 , 118, 45-61		79
350	The isotopic composition of authigenic chromium in anoxic marine sediments: A case study from the Cariaco Basin. <i>Earth and Planetary Science Letters</i> , 2014 , 407, 9-18	5.3	78
349	Coupled reductive and oxidative sulfur cycling in the phototrophic plate of a meromictic lake. <i>Geobiology</i> , 2014 , 12, 451-68	4.3	28
348	Redox heterogeneity of subsurface waters in the Mesoproterozoic ocean. <i>Geobiology</i> , 2014 , 12, 373-86	4.3	96
347	Evolution: a fixed-nitrogen fix in the early ocean?. 2014 , 24, R276-8		7
346	Ocean redox structure across the Late Neoproterozoic Oxygenation Event: A nitrogen isotope perspective. <i>Earth and Planetary Science Letters</i> , 2014 , 396, 1-13	5.3	82
345	Causes and consequences of mid-Proterozoic anoxia. 2015 , 42, 8538-8546		82
344	Ediacaran Marine Redox Heterogeneity and Early Animal Ecosystems. 2015, 5, 17097		47
343	The behavior of biologically important trace elements across the oxic/euxinic transition of meromictic Fayetteville Green Lake, New York, USA. <i>Geochimica Et Cosmochimica Acta</i> , 2015 , 165, 389-4	0 65	31
342	Late Proterozoic Transitions in Climate, Oxygen, and Tectonics, and the Rise of Complex Life. 2015 , 21, 47-82		9
341	Is the Neoproterozoic oxygen burst a supercontinent legacy?. Frontiers in Earth Science, 2015, 3,	3.5	5
340	Deep-water microbialites of the Mesoproterozoic Dismal Lakes Group: microbial growth, lithification, and implications for coniform stromatolites. <i>Geobiology</i> , 2015 , 13, 15-32	4.3	29
339	The evolution of the global selenium cycle: Secular trends in Se isotopes and abundances. <i>Geochimica Et Cosmochimica Acta</i> , 2015 , 162, 109-125	5.5	49

338	Sedimentology, chemostratigraphy, and stromatolites of lower Paleoproterozoic carbonates, Turee Creek Group, Western Australia. <i>Precambrian Research</i> , 2015 , 266, 194-211	3.9	21
337	Rise to modern levels of ocean oxygenation coincided with the Cambrian radiation of animals. 2015 , 6, 7142		198
336	Heterogeneous redox conditions and a shallow chemocline in the Mesoproterozoic ocean: Evidence from carbonBulfurIron relationships. <i>Precambrian Research</i> , 2015 , 257, 94-108	3.9	50
335	Marine redox conditions in the middle Proterozoic ocean and isotopic constraints on authigenic carbonate formation: Insights from the Chuanlinggou Formation, Yanshan Basin, North China. <i>Geochimica Et Cosmochimica Acta</i> , 2015 , 150, 90-105	5.5	57
334	Sulfur-cycling fossil bacteria from the 1.8-Ga Duck Creek Formation provide promising evidence of evolution's null hypothesis. <i>Proceedings of the National Academy of Sciences of the United States of America</i> , 2015 , 112, 2087-92	11.5	41
333	Connecting biodiversity and potential functional role in modern euxinic environments by microbial metagenomics. 2015 , 9, 1648-61		73
332	Uranium and molybdenum isotope evidence for an episode of widespread ocean oxygenation during the late Ediacaran Period. <i>Geochimica Et Cosmochimica Acta</i> , 2015 , 156, 173-193	5.5	179
331	Magnesium isotopic compositions of the Mesoproterozoic dolostones: Implications for Mg isotopic systematics of marine carbonates. <i>Geochimica Et Cosmochimica Acta</i> , 2015 , 164, 333-351	5.5	51
330	Global variability of chromium isotopes in seawater demonstrated by Pacific, Atlantic, and Arctic Ocean samples. <i>Earth and Planetary Science Letters</i> , 2015 , 423, 87-97	5.3	95
329	Statistical analysis of iron geochemical data suggests limited late Proterozoic oxygenation. 2015 , 523, 451-4		365
329 328			365 203
	523, 451-4		
328	523, 451-4 Trace Element Content of Sedimentary Pyrite in Black Shales. 2015, 110, 1389-1410 Germanium/silicon of the Ediacaran-Cambrian Laobao cherts: Implications for the bedded chert		203
328 327	Trace Element Content of Sedimentary Pyrite in Black Shales. 2015, 110, 1389-1410 Germanium/silicon of the Ediacaran-Cambrian Laobao cherts: Implications for the bedded chert formation and paleoenvironment interpretations. 2015, 16, 751-763	4-3	203
328 327 326	Trace Element Content of Sedimentary Pyrite in Black Shales. 2015, 110, 1389-1410 Germanium/silicon of the Ediacaran-Cambrian Laobao cherts: Implications for the bedded chert formation and paleoenvironment interpretations. 2015, 16, 751-763 Was the Ediacaran Cambrian radiation a unique evolutionary event?. 2015, 41, 1-15		203 35 26
328 327 326 325	Trace Element Content of Sedimentary Pyrite in Black Shales. 2015, 110, 1389-1410 Germanium/silicon of the Ediacaran-Cambrian Laobao cherts: Implications for the bedded chert formation and paleoenvironment interpretations. 2015, 16, 751-763 Was the Ediacaran@ambrian radiation a unique evolutionary event?. 2015, 41, 1-15 A public goods approach to major evolutionary innovations. <i>Geobiology</i> , 2015, 13, 308-15		203 35 26
328 327 326 325 324	Trace Element Content of Sedimentary Pyrite in Black Shales. 2015, 110, 1389-1410 Germanium/silicon of the Ediacaran-Cambrian Laobao cherts: Implications for the bedded chert formation and paleoenvironment interpretations. 2015, 16, 751-763 Was the Ediacaran Tambrian radiation a unique evolutionary event?. 2015, 41, 1-15 A public goods approach to major evolutionary innovations. <i>Geobiology</i> , 2015, 13, 308-15 High Molybdenum availability for evolution in a Mesoproterozoic lacustrine environment. 2015, 6, 6996		203 35 26 17 21

(2016-2015)

320	Mo marine geochemistry and reconstruction of ancient ocean redox states. <i>Science China Earth Sciences</i> , 2015 , 58, 2123-2133	4.6	13
319	Euxinic conditions recorded in the ca. 1.93 Ga Bravo Lake Formation, Nunavut (Canada): Implications for oceanic redox evolution. <i>Chemical Geology</i> , 2015 , 417, 148-162	4.2	13
318	Increase of seawater Mo inventory and ocean oxygenation during the early Cambrian. <i>Palaeogeography, Palaeoclimatology, Palaeoecology</i> , 2015 , 440, 621-631	2.9	27
317	Cycles of nutrient trace elements in the Phanerozoic ocean. 2015 , 28, 1282-1293		88
316	Carbon and Sulfur Cycling below the Chemocline in a Meromictic Lake and the Identification of a Novel Taxonomic Lineage in the FCB Superphylum, Candidatus Aegiribacteria. 2016 , 7, 598		26
315	Cyanobacterial Diazotrophy and Earth's Delayed Oxygenation. 2016 , 7, 1526		11
314	Mineralogical Diversity in Lake Pavin: Connections with Water Column Chemistry and Biomineralization Processes. 2016 , 6, 24		19
313	Oceanic oxygenation events in the anoxic Ediacaran ocean. <i>Geobiology</i> , 2016 , 14, 457-68	4.3	181
312	Arsenic stress after the Proterozoic glaciations. 2015 , 5, 17789		22
311	Cyanobacterial evolution during the Precambrian. 2016 , 15, 187-204		71
311	Cyanobacterial evolution during the Precambrian. 2016 , 15, 187-204 Powered by light: Phototrophy and photosynthesis in prokaryotes and its evolution. 2016 , 186-187, 99-	118	7 ¹
		118 4·3	
310	Powered by light: Phototrophy and photosynthesis in prokaryotes and its evolution. 2016 , 186-187, 99-Chromium-isotope signatures in scleractinian corals from the Rocas Atoll, Tropical South Atlantic.		34
310	Powered by light: Phototrophy and photosynthesis in prokaryotes and its evolution. 2016 , 186-187, 99-Chromium-isotope signatures in scleractinian corals from the Rocas Atoll, Tropical South Atlantic. <i>Geobiology</i> , 2016 , 14, 54-67 Sedimentary chromium isotopic compositions across the Cretaceous OAE2 at Demerara Rise Site	4.3	34
310 309 308	Powered by light: Phototrophy and photosynthesis in prokaryotes and its evolution. 2016 , 186-187, 99-Chromium-isotope signatures in scleractinian corals from the Rocas Atoll, Tropical South Atlantic. <i>Geobiology</i> , 2016 , 14, 54-67 Sedimentary chromium isotopic compositions across the Cretaceous OAE2 at Demerara Rise Site 1258. <i>Chemical Geology</i> , 2016 , 429, 85-92 No evidence for high atmospheric oxygen levels 1,400 million years ago. <i>Proceedings of the National</i>	4.3	34 43 31
310 309 308 307	Powered by light: Phototrophy and photosynthesis in prokaryotes and its evolution. 2016, 186-187, 99- Chromium-isotope signatures in scleractinian corals from the Rocas Atoll, Tropical South Atlantic. Geobiology, 2016, 14, 54-67 Sedimentary chromium isotopic compositions across the Cretaceous OAE2 at Demerara Rise Site 1258. Chemical Geology, 2016, 429, 85-92 No evidence for high atmospheric oxygen levels 1,400 million years ago. Proceedings of the National Academy of Sciences of the United States of America, 2016, 113, E2550-1 The chromium isotope composition of reducing and oxic marine sediments. Geochimica Et	4·3 4·2 11.5	34433133
310 309 308 307 306	Powered by light: Phototrophy and photosynthesis in prokaryotes and its evolution. 2016, 186-187, 99-Chromium-isotope signatures in scleractinian corals from the Rocas Atoll, Tropical South Atlantic. <i>Geobiology</i> , 2016, 14, 54-67 Sedimentary chromium isotopic compositions across the Cretaceous OAE2 at Demerara Rise Site 1258. <i>Chemical Geology</i> , 2016, 429, 85-92 No evidence for high atmospheric oxygen levels 1,400 million years ago. <i>Proceedings of the National Academy of Sciences of the United States of America</i> , 2016, 113, E2550-1 The chromium isotope composition of reducing and oxic marine sediments. <i>Geochimica Et Cosmochimica Acta</i> , 2016, 184, 1-19 Response of the Cr isotope proxy to Cretaceous Ocean Anoxic Event 2 in a pelagic carbonate	4.3 4.2 11.5	3443313358

302	Chromium isotope, REE and redox-sensitive trace element chemostratigraphy across the late Neoproterozoic Ghaub glaciation, Otavi Group, Namibia. <i>Precambrian Research</i> , 2016 , 286, 234-249	3.9	34
301	Basin redox and primary productivity within the Mesoproterozoic Roper Seaway. <i>Chemical Geology</i> , 2016 , 440, 101-114	4.2	64
300	Behaviors of trace elements in Neoarchean and Paleoproterozoic paleosols: Implications for atmospheric oxygen evolution and continental oxidative weathering. <i>Geochimica Et Cosmochimica Acta</i> , 2016 , 192, 203-219	5.5	9
299	Sedimentological perspectives on climatic, atmospheric and environmental change in the Neoproterozoic Era. 2016 , 63, 253-306		56
298	How Bacteria are Affected by Toxic Metal Release. 2016 , 253-270		1
297	RESEARCH FOCUS: Cracking the Neoproterozoic atmosphere?. 2016 , 44, 687-688		3
296	The evolution of Earth's biogeochemical nitrogen cycle. 2016 , 160, 220-239		160
295	Earth's oxygen cycle and the evolution of animal life. <i>Proceedings of the National Academy of Sciences of the United States of America</i> , 2016 , 113, 8933-8	11.5	145
294	Trace elements at the intersection of marine biological and geochemical evolution. 2016 , 163, 323-348		86
293	Molar tooth carbonates and benthic methane fluxes in Proterozoic oceans. 2016 , 7, 10317		17
293 292	Molar tooth carbonates and benthic methane fluxes in Proterozoic oceans. 2016 , 7, 10317 Phototrophic Microorganisms: The Basis of the Marine Food Web. 2016 , 57-97		17 2
		5.5	
292	Phototrophic Microorganisms: The Basis of the Marine Food Web. 2016 , 57-97 A comprehensive sulfur and oxygen isotope study of sulfur cycling in a shallow, hyper-euxinic	5.5	2
292	Phototrophic Microorganisms: The Basis of the Marine Food Web. 2016 , 57-97 A comprehensive sulfur and oxygen isotope study of sulfur cycling in a shallow, hyper-euxinic meromictic lake. <i>Geochimica Et Cosmochimica Acta</i> , 2016 , 189, 1-23 Empirical links between trace metal cycling and marine microbial ecology during a large		2 18
292 291 290	Phototrophic Microorganisms: The Basis of the Marine Food Web. 2016 , 57-97 A comprehensive sulfur and oxygen isotope study of sulfur cycling in a shallow, hyper-euxinic meromictic lake. <i>Geochimica Et Cosmochimica Acta</i> , 2016 , 189, 1-23 Empirical links between trace metal cycling and marine microbial ecology during a large perturbation to Earth's carbon cycle. <i>Earth and Planetary Science Letters</i> , 2016 , 449, 407-417 The Role of Microbial Electron Transfer in the Coevolution of the Biosphere and Geosphere. 2016 ,		2 18 59
292 291 290 289	Phototrophic Microorganisms: The Basis of the Marine Food Web. 2016, 57-97 A comprehensive sulfur and oxygen isotope study of sulfur cycling in a shallow, hyper-euxinic meromictic lake. <i>Geochimica Et Cosmochimica Acta</i> , 2016, 189, 1-23 Empirical links between trace metal cycling and marine microbial ecology during a large perturbation to Earth's carbon cycle. <i>Earth and Planetary Science Letters</i> , 2016, 449, 407-417 The Role of Microbial Electron Transfer in the Coevolution of the Biosphere and Geosphere. 2016, 70, 45-62 Geochemistry and Re®s geochronology of the organic-rich sedimentary rocks in the Jingtieshan		2 18 59 51
292 291 290 289 288	Phototrophic Microorganisms: The Basis of the Marine Food Web. 2016, 57-97 A comprehensive sulfur and oxygen isotope study of sulfur cycling in a shallow, hyper-euxinic meromictic lake. <i>Geochimica Et Cosmochimica Acta</i> , 2016, 189, 1-23 Empirical links between trace metal cycling and marine microbial ecology during a large perturbation to Earth's carbon cycle. <i>Earth and Planetary Science Letters</i> , 2016, 449, 407-417 The Role of Microbial Electron Transfer in the Coevolution of the Biosphere and Geosphere. 2016, 70, 45-62 Geochemistry and Rei geochronology of the organic-rich sedimentary rocks in the Jingtieshan Fellu deposit, North Qilian Mountains, NW China. 2016, 119, 65-77 Chromium isotope fractionation during subduction-related metamorphism, black shale weathering,	5:3	2 18 59 51 9

(2017-2016)

284	Extremely low oxygen concentration in mid-Proterozoic shallow seawaters. <i>Precambrian Research</i> , 2016 , 276, 145-157	3.9	62
283	Arsenic-induced phosphate limitation under experimental Early Proterozoic oceanic conditions. <i>Earth and Planetary Science Letters</i> , 2016 , 434, 52-63	5.3	7
282	Oxygen, facies, and secular controls on the appearance of Cryogenian and Ediacaran body and trace fossils in the Mackenzie Mountains of northwestern Canada. 2016 , 128, 558-575		44
281	Geochronological and geochemical studies of the metasedimentary rocks and diabase from the Jingtieshan deposit, North Qilian, NW China: Constraints on the associated banded iron formations. 2016 , 73, 42-58		21
280	Equable end Mesoproterozoic climate in the absence of high CO2. 2017 , 45, 231-234		24
279	Atmospheric oxygen regulation at low Proterozoic levels by incomplete oxidative weathering of sedimentary organic carbon. 2017 , 8, 14379		91
278	Chromium isotope systematics in the Connecticut River. Chemical Geology, 2017, 456, 98-111	4.2	56
277	Molybdenum speciation and burial pathway in weakly sulfidic environments: Insights from XAFS. <i>Geochimica Et Cosmochimica Acta</i> , 2017 , 206, 18-29	5.5	50
276	Tracking the onset of Phanerozoic-style redox-sensitive trace metal enrichments: New results from basal Ediacaran post-glacial strata in NW Canada. <i>Chemical Geology</i> , 2017 , 457, 24-37	4.2	26
275	Perspectives on Proterozoic surface ocean redox from iodine contents in ancient and recent carbonate. <i>Earth and Planetary Science Letters</i> , 2017 , 463, 159-170	5.3	119
274	False Negatives for Remote Life Detection on Ocean-Bearing Planets: Lessons from the Early Earth. 2017 , 17, 287-297		83
273	Microbe-clay interactions as a mechanism for the preservation of organic matter and trace metal biosignatures in black shales. <i>Chemical Geology</i> , 2017 , 459, 75-90	4.2	27
272	Transient deep-water oxygenation in the early Cambrian Nanhua Basin, South China. <i>Geochimica Et Cosmochimica Acta</i> , 2017 , 210, 42-58	5.5	53
271	Uranium isotope compositions of mid-Proterozoic black shales: Evidence for an episode of increased ocean oxygenation at 1.36 Ga and evaluation of the effect of post-depositional hydrothermal fluid flow. <i>Precambrian Research</i> , 2017 , 298, 187-201	3.9	45
270	Whole rock and discrete pyrite geochemistry as complementary tracers of ancient ocean chemistry: An example from the Neoproterozoic Doushantuo Formation, China. <i>Geochimica Et Cosmochimica Acta</i> , 2017 , 216, 201-220	5.5	44
269	A theory of atmospheric oxygen. <i>Geobiology</i> , 2017 , 15, 366-384	4.3	55
268	Marine redox evolution in the early Cambrian Yangtze shelf margin area: evidence from trace elements, nitrogen and sulphur isotopes. <i>Geological Magazine</i> , 2017 , 154, 1344-1359	2	11
267	Metabolic evolution and the self-organization of ecosystems. <i>Proceedings of the National Academy of Sciences of the United States of America</i> , 2017 , 114, E3091-E3100	11.5	79

266	Marine redox conditions during deposition of Late Ordovician and Early Silurian organic-rich mudrocks in the Siljan ring district, central Sweden. <i>Chemical Geology</i> , 2017 , 457, 75-94	4.2	30	
265	Atmospheric oxygenation driven by unsteady growth of the continental sedimentary reservoir. <i>Earth and Planetary Science Letters</i> , 2017 , 460, 68-75	5.3	42	
264	Micropaleontology of the lower Mesoproterozoic Roper Group, Australia, and implications for early eukaryotic evolution. 2017 , 91, 199-229		74	
263	Evolution of the global phosphorus cycle. 2017 , 541, 386-389		262	
262	A molybdenum-isotope perspective on Phanerozoic deoxygenation events. 2017 , 10, 721-726		48	
261	The onset of widespread marine red beds and the evolution of ferruginous oceans. 2017 , 8, 399		51	
260	Heterogenous oceanic redox conditions through the Ediacaran-Cambrian boundary limited the metazoan zonation. 2017 , 7, 8550		20	
259	Recurrent horizontal transfer of arsenite methyltransferase genes facilitated adaptation of life to arsenic. 2017 , 7, 7741		40	
258	Temporal record of osmium concentrations and 1870s/1880s in organic-rich mudrocks: Implications for the osmium geochemical cycle and the use of osmium as a paleoceanographic tracer. <i>Geochimica Et Cosmochimica Acta</i> , 2017 , 216, 221-241	5.5	9	
257	A new estimate of detrital redox-sensitive metal concentrations and variability in fluxes to marine sediments. <i>Geochimica Et Cosmochimica Acta</i> , 2017 , 215, 337-353	5.5	65	
256	Thallium-isotopic compositions of euxinic sediments as a proxy for global manganese-oxide burial. <i>Geochimica Et Cosmochimica Acta</i> , 2017 , 213, 291-307	5.5	44	
255	Iron formations: A global record of Neoarchaean to Palaeoproterozoic environmental history. 2017 , 172, 140-177		190	
254	Redox fluctuations in the Early Ordovician oceans: An insight from chromium stable isotopes. <i>Chemical Geology</i> , 2017 , 448, 1-12	4.2	32	
253	Chromium isotopic composition of core-top planktonic foraminifera. <i>Geobiology</i> , 2017 , 15, 51-64	4.3	27	
252	Spatial and temporal trends in Precambrian nitrogen cycling: A Mesoproterozoic offshore nitrate minimum. <i>Geochimica Et Cosmochimica Acta</i> , 2017 , 198, 315-337	5.5	50	
251	Patterns of local and global redox variability during the Cenomanian uronian Boundary Event (Oceanic Anoxic Event 2) recorded in carbonates and shales from central Italy. 2017 , 64, 168-185		36	
250	16 Good Golly, Why Moly? THE STABLE ISOTOPE GEOCHEMISTRY OF MOLYBDENUM. 2017 ,		3	
249	10 Chromium Isotope Geochemistry. 2017 ,		1	

248	Photoferrotrophy: Remains of an Ancient Photosynthesis in Modern Environments. 2017, 8, 323		42
247	Stratiform siderites from the Mesoproterozoic Xiamaling Formation in North China: Genesis and environmental implications. 2018 , 58, 1-15		23
246	Earth: Atmospheric Evolution of a Habitable Planet. 2018 , 1-37		1
245	Nitrogen fixation sustained productivity in the wake of the Palaeoproterozoic Great Oxygenation Event. 2018 , 9, 978		27
244	Modern rather than Mesoarchaean oxidative weathering responsible for the heavy stable Cr isotopic signatures of the 2.95 Ga old ljzermijn iron formation (South Africa). <i>Geochimica Et Cosmochimica Acta</i> , 2018 , 228, 157-189	5.5	55
243	Manganese and iron geochemistry in sediments underlying the redox-stratified Fayetteville Green Lake. <i>Geochimica Et Cosmochimica Acta</i> , 2018 , 231, 50-63	5.5	33
242	Trace Elements Characteristics of Black Shales from the Ediacaran Doushantuo Formation, Hubei Province, South China: Implications for Redox and Open vs. Restricted Basin Conditions. 2018 , 29, 342-3	352	11
241	What the \sim 1.4 Ga Xiamaling Formation can and cannot tell us about the mid-Proterozoic ocean. <i>Geobiology</i> , 2018 , 16, 219-236	4.3	41
240	A model for the oceanic mass balance of rhenium and implications for the extent of Proterozoic ocean anoxia. <i>Geochimica Et Cosmochimica Acta</i> , 2018 , 227, 75-95	5.5	42
239	Tellurium, selenium and cobalt enrichment in Neoproterozoic black shales, Gwna Group, UK: Deep marine trace element enrichment during the Second Great Oxygenation Event. <i>Terra Nova</i> , 2018 , 30, 244-253	3	9
238	Anoxic to suboxic Mesoproterozoic ocean: Evidence from iron isotope and geochemistry of siderite in the Banded Iron Formations from North Qilian, NW China. <i>Precambrian Research</i> , 2018 , 307, 115-124	3.9	17
237	Disequilibrium biosignatures over Earth history and implications for detecting exoplanet life. 2018 , 4, eaao5747		72
236	Behaviour of chromium isotopes in the eastern sub-tropical Atlantic Oxygen Minimum Zone. <i>Geochimica Et Cosmochimica Acta</i> , 2018 , 236, 41-59	5.5	38
235	Controls on O2Production in Cyanobacterial Mats and Implications for Earth's Oxygenation. 2018 , 46, 123-147		22
234	Limitations on Limitation. Global Biogeochemical Cycles, 2018, 32, 486-496	5.9	32
233	Evidence for episodic oxygenation in a weakly redox-buffered deep mid-Proterozoic ocean. <i>Chemical Geology</i> , 2018 , 483, 581-594	4.2	52
232	Ichnofabrics and chemostratigraphy argue against persistent anoxia during the Upper Kellwasser Event in New York State. <i>Palaeogeography, Palaeoclimatology, Palaeoecology,</i> 2018 , 490, 178-190	2.9	17
231	Evidence for local and global redox conditions at an Early Ordovician (Tremadocian) mass extinction. <i>Earth and Planetary Science Letters</i> , 2018 , 481, 125-135	5.3	33

230	Fe isotopes of a 2.4 Ga hematite-rich IF constrain marine redox conditions around the GOE. <i>Precambrian Research</i> , 2018 , 305, 218-235	3.9	12
229	Chromium isotope fractionation in ferruginous sediments. <i>Geochimica Et Cosmochimica Acta</i> , 2018 , 223, 198-215	5.5	16
228	Carbonaceous biosignatures of the earliest putative macroscopic multicellular eukaryotes from 1630 Ma Tuanshanzi Formation, north China. <i>Precambrian Research</i> , 2018 , 304, 99-109	3.9	18
227	Silicon and chromium stable isotopic systematics during basalt weathering and lateritisation: A comparison of variably weathered basalt profiles in the Deccan Traps, India. 2018 , 314, 190-204		24
226	Earth: Atmospheric Evolution of a Habitable Planet. 2018 , 2817-2853		3
225	Stepwise oxygenation of the Paleozoic atmosphere. 2018 , 9, 4081		85
224	Mineral Facilitated Horizontal Gene Transfer: A New Principle for Evolution of Life?. 2018 , 9, 2217		7
223	Shallow water anoxia in the Mesoproterozoic ocean: Evidence from the Bashkir Meganticlinorium, Southern Urals. <i>Precambrian Research</i> , 2018 , 317, 196-210	3.9	23
222	Nitrogen isotope constraints on the early Ediacaran ocean redox structure. <i>Geochimica Et Cosmochimica Acta</i> , 2018 , 240, 220-235	5.5	32
221	Oxygenation variations in the atmosphere and shallow seawaters of the Yangtze Platform during the Ediacaran Period: Clues from Cr-isotope and Ce-anomaly in carbonates. <i>Precambrian Research</i> , 2018 , 313, 78-90	3.9	34
220	Dwindling vanadium in seawater during the early Cambrian, South China. <i>Chemical Geology</i> , 2018 , 492, 20-29	4.2	17
219	Stepwise oxygenation of early Cambrian ocean controls early metazoan diversification. <i>Palaeogeography, Palaeoclimatology, Palaeoecology</i> , 2018 , 504, 86-103	2.9	19
218	Contrasting MoD enrichments of the basal Datangpo Formation in South China: Implications for the Cryogenian interglacial ocean redox. <i>Precambrian Research</i> , 2018 , 315, 66-74	3.9	18
217	The Temporal and Environmental Context of Early Animal Evolution: Considering All the Ingredients of an "Explosion". 2018 , 58, 605-622		51
216	Dynamic oxygen and coupled biological and ecological innovation during the second wave of the Ediacara Biota. 2018 , 2, 223-233		16
215	Triple oxygen isotope evidence for limited mid-Proterozoic primary productivity. 2018 , 559, 613-616		101
214	Encyclopedia of Geochemistry. Encyclopedia of Earth Sciences Series, 2018, 719-721	O	
213	Highly fractionated chromium isotopes in Mesoproterozoic-aged shales and atmospheric oxygen. 2018 , 9, 2871		91

212	Evaluation of phosphate-uptake mechanisms by Fe(III) (oxyhydr)oxides in Early Proterozoic oceanic conditions. 2018 , 15, 18		7
211	Ocean Redox State at 2500-500 Ma: Modern Concepts. 2018 , 53, 190-211		7
210	Authigenic chromium enrichments in Proterozoic ironstones. 2018 , 372, 25-43		6
209	Mid-Proterozoic redox evolution and the possibility of transient oxygenation events. 2018 , 2, 235-245		24
208	Marine ferromanganese oxide: A potentially important sink of light chromium isotopes?. <i>Chemical Geology</i> , 2018 , 495, 90-103	4.2	19
207	Nitrous oxide from chemodenitrification: A possible missing link in the Proterozoic greenhouse and the evolution of aerobic respiration. <i>Geobiology</i> , 2018 , 16, 597-609	4.3	23
206	Extensive marine anoxia during the terminal Ediacaran Period. 2018, 4, eaan8983		82
205	The role of pH on Cr(VI) partitioning and isotopic fractionation during its incorporation in calcite. <i>Geochimica Et Cosmochimica Acta</i> , 2019 , 265, 520-532	5.5	14
204	Multiple negative molybdenum isotope excursions in the Doushantuo Formation (South China) fingerprint complex redox-related processes in the Ediacaran Nanhua Basin. <i>Geochimica Et Cosmochimica Acta</i> , 2019 , 261, 191-209	5.5	32
203	Shallow-marine ironstones formed by microaerophilic iron-oxidizing bacteria in terminal Paleoproterozoic. 2019 , 76, 1-18		14
202	Subtle Cr isotope signals track the variably anoxic Cryogenian interglacial period with voluminous manganese accumulation and decrease in biodiversity. 2019 , 9, 15056		4
201	Transect variations and controlling factors of redox-sensitive trace element compositions of surface sediments in the South China Sea. 2019 , 190, 103978		1
200	A paleosol record of the evolution of Cr redox cycling and evidence for an increase in atmospheric oxygen during the Neoproterozoic. <i>Geobiology</i> , 2019 , 17, 579-593	4.3	14
199	Pyrite trace-element and sulfur isotope geochemistry of paleo-mesoproterozoic McArthur Basin: Proxy for oxidative weathering. 2019 , 104, 1256-1272		16
198	Chromium isotopes in marine hydrothermal sediments. <i>Chemical Geology</i> , 2019 , 529, 119286	4.2	10
197	The impact of ionic strength on the proton reactivity of clay minerals. Chemical Geology, 2019, 529, 119	2.9.4	20
196	The History, Relevance, and Applications of the Periodic System in Geochemistry. 2019, 111		
195	A multi-basin redox reconstruction for the Miocene Monterey Formation, California, USA. <i>Palaeogeography, Palaeoclimatology, Palaeoecology</i> , 2019 , 520, 114-127	2.9	6

194	Linking the Bitter Springs carbon isotope anomaly and early Neoproterozoic oxygenation through I/[Ca + Mg] ratios. <i>Chemical Geology</i> , 2019 , 524, 119-135	4.2	14
193	A tectonically driven Ediacaran oxygenation event. 2019 , 10, 2690		21
192	Uranium isotope evidence for limited euxinia in mid-Proterozoic oceans. <i>Earth and Planetary Science Letters</i> , 2019 , 521, 150-157	5.3	37
191	The Great Oxygenation Event. 2019 , 129-154		1
190	Evolution of cellular metabolism and the rise of a globally productive biosphere. 2019 , 140, 172-187		10
189	Chromium isotope cycling in the water column and sediments of the Peruvian continental margin. <i>Geochimica Et Cosmochimica Acta</i> , 2019 , 257, 224-242	5.5	20
188	Species-Dependent Chromium Isotope Fractionation Across the Eastern Tropical North Pacific Oxygen Minimum Zone. 2019 , 20, 2499		4
187	Cr isotopic insights into ca. 1.9 Ga oxidative weathering of the continents using the Beaverlodge Lake paleosol, Northwest Territories, Canada. <i>Geobiology</i> , 2019 , 17, 467-489	4.3	9
186	Chemostratigraphy of the Mesoproterozoic Shennongjia Group, Yangtze Craton (South China): Implications for oxidized shallow seawaters. 2019 , 179, 399-415		9
185	Claypool continued: Extending the isotopic record of sedimentary sulfate. <i>Chemical Geology</i> , 2019 , 513, 200-225	4.2	59
184	Dynamic interaction between basin redox and the biogeochemical nitrogen cycle in an unconventional Proterozoic petroleum system. 2019 , 9, 5200		9
183	Atmosphere oxygen cycling through the Proterozoic and Phanerozoic. 2019 , 54, 485-506		46
182	Oxygen Reductases in Alphaproteobacterial Genomes: Physiological Evolution From Low to High Oxygen Environments. 2019 , 10, 499		19
181	Heterogeneity and incorporation of chromium isotopes in recent marine molluscs (Mytilus). <i>Geobiology</i> , 2019 , 17, 417-435	4.3	19
180	Microbial diversity involved in iron and cryptic sulfur cycling in the ferruginous, low-sulfate waters of Lake Pavin. 2019 , 14, e0212787		25
179	Primary Productivity Was Limited by Electron Donors Prior to the Advent of Oxygenic Photosynthesis. 2019 , 124, 211-226		37
178	Mechanistic Links Between the Sedimentary Redox Cycle and Marine Acid-Base Chemistry. 2019 , 20, 5968-5978		2
177	Spatial Variations of Trace Metals and Their Complexation Behavior with DOM in the Water of Dianchi Lake, China. 2019 , 16,		3

(2020-2019)

176	Links between early Paleozoic oxygenation and the Great Ordovician Biodiversification Event (GOBE): A review. 2019 , 28, 37-50		18
175	Absence of biomarker evidence for early eukaryotic life from the Mesoproterozoic Roper Group: Searching across a marine redox gradient in mid-Proterozoic habitability. <i>Geobiology</i> , 2019 , 17, 247-260	4.3	25
174	Cr isotope systematics in the Connecticut River estuary. <i>Chemical Geology</i> , 2019 , 506, 29-39	4.2	17
173	Biotic, geochemical and environmental changes through the early Sheinwoodian (Wenlock, Silurian) carbon isotope excursion (ESCIE), Buttington Quarry, Wales. <i>Palaeogeography, Palaeoclimatology,</i> 214, 305-325	2.9	4
172	Global-ocean redox variations across the Smithian-Spathian boundary linked to concurrent climatic and biotic changes. 2019 , 195, 147-168		23
171	The selective pressures on the microbial community in a metal-contaminated aquifer. 2019 , 13, 937-949		27
170	A sluggish mid-Proterozoic biosphere and its effect on Earth's redox balance. <i>Geobiology</i> , 2019 , 17, 3-11 4	4.3	45
169	Redox-Sensitive Metals. 2019, 323-328		
168	Antagonistic co-limitation through ion promiscuity - On the metal sensitivity of Thalassiosira oceanica under phosphorus stress. 2020 , 699, 134080		1
167	Reconstruction of nearshore chemical conditions in the Mesoproterozoic: evidence from red and grey beds of the Yangzhuang formation, North China Craton. 2020 , 62, 1433-1449		3
166	Lower Triassic carbonate 238U record demonstrates expanded oceanic anoxia during Smithian Thermal Maximum and improved ventilation during Smithian-Spathian boundary cooling event. Palaeogeography, Palaeoclimatology, Palaeoecology, 2020, 539, 109393	2.9	13
165	Mo-Ni and organic carbon isotope signatures of the mid-late Mesoproterozoic oxygenation. 2020 , 191, 104201		3
164	Carbonates before skeletons: A database approach. 2020 , 201, 103065		20
163	Spatiotemporal redox heterogeneity and transient marine shelf oxygenation in the Mesoproterozoic ocean. <i>Geochimica Et Cosmochimica Acta</i> , 2020 , 270, 201-217	5.5	20
162	Estimating ancient seawater isotope compositions and global ocean redox conditions by coupling the molybdenum and uranium isotope systems of euxinic organic-rich mudrocks. <i>Geochimica Et Cosmochimica Acta</i> , 2020 , 290, 76-103	5.5	14
161	Cadmium adsorption to clay-microbe aggregates: Implications for marine heavy metals cycling. <i>Geochimica Et Cosmochimica Acta</i> , 2020 , 290, 124-136	5.5	25
160	The global explosion of eukaryotic algae: The potential role of phosphorus?. 2020 , 15, e0234372		2
159	Tracking the evolution of seawater Mo isotopes through the Ediacaran Cambrian transition. **Precambrian Research*, 2020*, 350, 105929** 3	3.9	7

158	Versatile cyanobacteria control the timing and extent of sulfide production in a Proterozoic analog microbial mat. 2020 , 14, 3024-3037		8
157	Geochemical signatures of redepositional environments: The Namibian continental margin. 2020 , 429, 106316		1
156	Geochemical fingerprints of seawater in the Late Mesoproterozoic Midcontinent Rift, North America: Life at the marine-land divide. <i>Chemical Geology</i> , 2020 , 553, 119812	4.2	3
155	Thallium isotope ratios in shales from South China and northwestern Canada suggest widespread O2 accumulation in marine bottom waters was an uncommon occurrence during the Ediacaran Period. <i>Chemical Geology</i> , 2020 , 557, 119856	4.2	10
154	Using modern low-oxygen marine ecosystems to understand the nitrogen cycle of the Paleo- and Mesoproterozoic oceans. 2021 , 23, 2801-2822		1
153	On the use of models in understanding the rise of complex life. 2020 , 10, 20200018		4
152	Molybdenum Isotope Constraints on the Origin of Vanadium Hyper-Enrichments in Ediacaran Phanerozoic Marine Mudrocks. 2020 , 10, 1075		2
151	The biogeochemistry of ferruginous lakes and past ferruginous oceans. 2020 , 211, 103430		7
150	A phylogenetically novel cyanobacterium most closely related to Gloeobacter. 2020 , 14, 2142-2152		11
149	Marine redox variability from Baltica during extinction events in the latest Ordovician arly Silurian. <i>Palaeogeography, Palaeoclimatology, Palaeoecology</i> , 2020 , 554, 109792	2.9	15
148	Reconciling proxy records and models of Earth's oxygenation during the Neoproterozoic and Palaeozoic. 2020 , 10, 20190137		19
147	Integrated sedimentary, biotic, and paleoredox dynamics from multiple localities in southern Laurentia during the late Silurian (Ludfordian) extinction event. <i>Palaeogeography, Palaeoecology</i> , 2020 , 553, 109799	2.9	6
146	Molybdenum geochemistry in salt marsh pond sediments. <i>Geochimica Et Cosmochimica Acta</i> , 2020 , 284, 75-91	5.5	7
145	Palaeoproterozoic oxygenated oceans following the Lomagundillatuli Event. 2020 , 13, 302-306		25
144	Mission to Planet Earth: The First Two Billion Years. 2020 , 216, 1		9
143	Associations between redox-sensitive trace metals and microbial communities in a Proterozoic ocean analogue. <i>Geobiology</i> , 2020 , 18, 462-475	4.3	3
142	Biogeochemical cycle of chromium isotopes at the modern Earth's surface and its applications as a paleo-environment proxy. <i>Chemical Geology</i> , 2020 , 541, 119570	4.2	18
141	Coupled Nitrate and Phosphate Availability Facilitated the Expansion of Eukaryotic Life at Circa 1.56 Ga. 2020 , 125, e2019JG005487		9

140	On the co-evolution of surface oxygen levels and animals. <i>Geobiology</i> , 2020 , 18, 260-281	4.3	43
139	Surface ocean nitrate-limitation in the aftermath of Marinoan snowball Earth: Evidence from the Ediacaran Doushantuo Formation in the western margin of the Yangtze Block, South China. <i>Precambrian Research</i> , 2020 , 347, 105846	3.9	3
138	Uranium Isotope Fractionation in Non-sulfidic Anoxic Settings and the Global Uranium Isotope Mass Balance. <i>Global Biogeochemical Cycles</i> , 2020 , 34, e2020GB006649	5.9	21
137	Mesoproterozoic paleo-redox changes during 1500¶400 Ma in the Yanshan Basin, North China. <i>Precambrian Research</i> , 2020 , 347, 105835	3.9	6
136	Niche expansion for phototrophic sulfur bacteria at the Proterozoic-Phanerozoic transition. <i>Proceedings of the National Academy of Sciences of the United States of America</i> , 2020 , 117, 17599-17606	5 ^{11.5}	16
135	Sequence stratigraphy in organic-rich marine mudstone successions using chemostratigraphic datasets. 2020 , 203, 103137		11
134	Behaviour of chromium and chromium isotopes during estuarine mixing in the Beaulieu Estuary, UK. <i>Earth and Planetary Science Letters</i> , 2020 , 536, 116166	5.3	11
133	Microbial feedbacks optimize ocean iron availability. <i>Proceedings of the National Academy of Sciences of the United States of America</i> , 2020 , 117, 4842-4849	11.5	12
132	Rhenium-Osmium isotope systematics of an Early Mesoproterozoic SEDEX polymetallic pyrite deposit in the North China Craton: Implications for geological significance and the marine osmium isotopic record. 2020 , 117, 103331		3
131	Uranium reduction and isotopic fractionation in reducing sediments: Insights from reactive transport modeling. <i>Geochimica Et Cosmochimica Acta</i> , 2020 , 287, 65-92	5.5	20
130	Inverse correlation between the molybdenum and uranium isotope compositions of Upper Devonian black shales caused by changes in local depositional conditions rather than global ocean redox variations. <i>Geochimica Et Cosmochimica Acta</i> , 2020 , 287, 141-164	5.5	14
129	Molybdenum isotope and trace metal signals in an iron-rich Mesoproterozoic ocean: A snapshot from the Vindhyan Basin, India. <i>Precambrian Research</i> , 2020 , 343, 105718	3.9	12
128	Evidence for elevated and variable atmospheric oxygen in the Precambrian. <i>Precambrian Research</i> , 2020 , 343, 105722	3.9	21
127	Persistent global marine euxinia in the early Silurian. 2020 , 11, 1804		34
126	Geochemical signatures of transgressive shale intervals from the 811 Ma Fifteenmile Group in Yukon, Canada: Disentangling sedimentary redox cycling from weathering alteration. <i>Geochimica Et Cosmochimica Acta</i> , 2020 , 280, 161-184	5.5	4
125	New insights into Paleoproterozoic surficial conditions revealed by 1.85 Ga corestone-rich saprolith. <i>Chemical Geology</i> , 2020 , 545, 119621	4.2	3
124	Enhanced chemical weathering triggered an expansion of euxinic seawater in the aftermath of the Sturtian glaciation. <i>Earth and Planetary Science Letters</i> , 2020 , 539, 116244	5.3	16
123	Investigation of tungstate thiolation reaction kinetics and sedimentary molybdenum/tungsten enrichments: Implication for tungsten speciation in sulfidic waters and possible applications for paleoredox studies. <i>Geochimica Et Cosmochimica Acta</i> , 2020 , 287, 277-295	5.5	16

122	Surge of ore metals in seawater and increased bio-activity: a tracer of VHMS mineralization in Archaean successions, Yilgarn Craton, Western Australia. 2021 , 56, 643-664		1
121	Radiation of nitrogen-metabolizing enzymes across the tree of life tracks environmental transitions in Earth history. <i>Geobiology</i> , 2021 , 19, 18-34	4.3	7
12 0	Evolution of Earth's Atmosphere. 2021 , 571-584		2
119	Assessing the Effect of Large Igneous Provinces on Global Oceanic Redox Conditions Using Non-traditional Metal Isotopes (Molybdenum, Uranium, Thallium). 2021 , 305-323		1
118	The Chromium Isotope System as a Tracer of Ocean and Atmosphere Redox. 2021,		5
117	A late Paleoproterozoic (1.74´Ga) deep-sea, low-temperature, iron-oxidizing microbial hydrothermal vent community from Arizona, USA. <i>Geobiology</i> , 2021 , 19, 228-249	4.3	6
116	The Nickel isotope composition of the authigenic sink and the diagenetic flux in modern oceans. <i>Chemical Geology</i> , 2021 , 563, 120050	4.2	4
115	Heterogeneous oxygenation coupled with low phosphorus bio-availability delayed eukaryotic diversification in Mesoproterozoic oceans: Evidence from the ca 1.46 Ga Hongshuizhuang Formation of North China. <i>Precambrian Research</i> , 2021 , 354, 106050	3.9	2
114	Cracking the superheavy pyrite enigma: possible roles of volatile organosulfur compound emission. 2021 , 8, nwab034		5
113	Spatial heterogeneity of redox-sensitive trace metal enrichments in upper Ediacaran anoxic black shales. 2021 , 178, jgs2020-234		3
112	A transient swing to higher oxygen levels in the atmosphere and oceans at ~1.4 Ga. <i>Precambrian Research</i> , 2021 , 354, 106058	3.9	12
111	Oceanic water chemistry evolution and its implications for post-glacial black shale formation: Insights from the Cryogenian Datangpo Formation, South China. <i>Chemical Geology</i> , 2021 , 566, 120083	4.2	4
110	Heterogeneous redox evolution of the Meso-Neoproterozoic ocean: Insights from eastern China. <i>Palaeogeography, Palaeoclimatology, Palaeoecology</i> , 2021 , 567, 110304	2.9	2
109	Pulsed oxygenation events drove progressive oxygenation of the early Mesoproterozoic ocean. <i>Earth and Planetary Science Letters</i> , 2021 , 559, 116754	5.3	4
108	Revisiting stepwise ocean oxygenation with authigenic barium enrichments in marine mudrocks. 2021 , 49, 1059-1063		5
107	Bioactive trace metals and their isotopes as paleoproductivity proxies: An assessment using GEOTRACES-era data. <i>Global Biogeochemical Cycles</i> , e2020GB006814	5.9	6
106	A Pulsed Oxygenation in Terminal Paleoproterozoic Ocean: Evidence From the Transition Between the Chuanlinggou and Tuanshanzi Formations, North China. 2021 , 22, e2020GC009612		4
105	Iron and sulfur cycling in the cGENIE.muffin Earth system model (v0.9.21). 2021 , 14, 2713-2745		3

(2021-2021)

104	The uranium isotopic record of shales and carbonates through geologic time. <i>Geochimica Et Cosmochimica Acta</i> , 2021 , 300, 164-191	5.5	9
103	Hexagonal magnetite in Algoma-type banded iron formations of the ca. 2.52 Ga Baizhiyan Formation (Wutai Group, North China): evidence for a green rust precursor?. 2021 ,		О
102	Precambrian and early Cambrian palaeobiology of India: Quo Vadis. 2021, 87, 199-233		1
101	A quantification of the effect of diagenesis on the paleoredox record in mid-Proterozoic sedimentary rocks. 2021 , 49, 1143-1147		1
100	Restricted Oxygen-Deficient Basins on the Northern European Epicontinental Shelf Across the Toarcian Carbon Isotope Excursion Interval. 2021 , 36, e2020PA004207		3
99	Depositional age and geochemistry of the 2.44\(\textit{2.32}\) Ga Granular Iron Formation in the Songshan Group, North China Craton: Tracing the effects of atmospheric oxygenation on continental weathering and seawater environment. <i>Precambrian Research</i> , 2021 , 357, 106142	3.9	4
98	Benthic redox conditions and nutrient dynamics in the ca. 2.1 Ga Franceville sub-basin. <i>Precambrian Research</i> , 2021 , 360, 106234	3.9	2
97	A long-term record of early to mid-Paleozoic marine redox change. 2021 , 7,		10
96	Chromium isotope heterogeneity on a modern carbonate platform. Chemical Geology, 2021, 573, 12022	74.2	4
95	The environmental context of carbonaceous compressions and implications for organism preservation 1.40 Ga and 0.63 Ga. <i>Palaeogeography, Palaeoclimatology, Palaeoecology</i> , 2021 , 573, 11044	1 3 .9	4
94	Purple sulfur bacteria fix N via molybdenum-nitrogenase in a low molybdenum Proterozoic ocean analogue. 2021 , 12, 4774		3
93	Molybdenum as a Paleoredox Proxy: Past, Present, and Future. 2021 ,		O
92	Vanadium isotope evidence for expansive ocean euxinia during the appearance of early Ediacara biota. <i>Earth and Planetary Science Letters</i> , 2021 , 567, 117007	5.3	1
91	Multiple Hydrothermal Iron-Formation Upgrading Events in Southeastern SB Francisco Craton. 000-000		1
90	Possible link between Earth rotation rate and oxygenation. 2021 , 14, 564-570		8
89	Oxygenation, Life, and the Planetary System during Earth's Middle History: An Overview. 2021 , 21, 906-	923	14
88	Chromium isotope fractionation during black shale weathering and its environmental implications. 2021 , 783, 147126		2
87	The History of Ocean Oxygenation. 2021 ,		2

86	Sulfidic anoxia in the oceans during the Late Ordovician mass extinctions linsights from molybdenum and uranium isotopic global redox proxies. 2021 , 220, 103748		6
85	Chromium stable isotope geochemistry in the Mobile Bay Estuary. <i>Chemical Geology</i> , 2021 , 584, 120530	4.2	O
84	Redox-Controlled Ammonium Storage and Overturn in Ediacaran Oceans. <i>Frontiers in Earth Science</i> , 2021 , 9,	3.5	
83	New constraints on mid-Proterozoic ocean redox from stable thallium isotope systematics of black shales. <i>Geochimica Et Cosmochimica Acta</i> , 2021 , 315, 185-185	5.5	1
82	Early Neoproterozoic oxygenation dynamics along the northern margin of the West African Craton, Anti-Atlas Mountains, Morocco. <i>Chemical Geology</i> , 2021 , 581, 120404	4.2	О
81	Reconciling evidence of oxidative weathering and atmospheric anoxia on Archean Earth. 2021 , 7, eabj0	108	5
80	Decoupled Cr, Mo, and U records of the Hongshuizhuang Formation, North China: Constraints on the Mesoproterozoic ocean redox. 2021 , 132, 105243		O
79	Redox dynamics of later Cambrian oceans. <i>Palaeogeography, Palaeoclimatology, Palaeoecology</i> , 2021 , 581, 110623	2.9	6
78	Breaking the Boring Billion. 2021 , 487-501		2
77	Recent Advances in Geochemical Paleo-Oxybarometers. 2021 , 49,		6
77 76	Recent Advances in Geochemical Paleo-Oxybarometers. 2021, 49, Encyclopedia of Geochemistry. Encyclopedia of Earth Sciences Series, 2016, 1-4	0	1
		0	
76	Encyclopedia of Geochemistry. <i>Encyclopedia of Earth Sciences Series</i> , 2016 , 1-4		1
76 75	Encyclopedia of Geochemistry. <i>Encyclopedia of Earth Sciences Series</i> , 2016 , 1-4 Encyclopedia of Geochemistry. <i>Encyclopedia of Earth Sciences Series</i> , 2018 , 947-950 Uranium isotopes in marine carbonates as a global ocean paleoredox proxy: A critical review.	0	1
76 75 74	Encyclopedia of Geochemistry. Encyclopedia of Earth Sciences Series, 2016, 1-4 Encyclopedia of Geochemistry. Encyclopedia of Earth Sciences Series, 2018, 947-950 Uranium isotopes in marine carbonates as a global ocean paleoredox proxy: A critical review. Geochimica Et Cosmochimica Acta, 2020, 287, 27-49 Delayed Neoproterozoic oceanic oxygenation: Evidence from Mo isotopes of the Cryogenian	o 5-5	1 1 30
76 75 74 73	Encyclopedia of Geochemistry. Encyclopedia of Earth Sciences Series, 2016, 1-4 Encyclopedia of Geochemistry. Encyclopedia of Earth Sciences Series, 2018, 947-950 Uranium isotopes in marine carbonates as a global ocean paleoredox proxy: A critical review. Geochimica Et Cosmochimica Acta, 2020, 287, 27-49 Delayed Neoproterozoic oceanic oxygenation: Evidence from Mo isotopes of the Cryogenian Datangpo Formation. Precambrian Research, 2018, 319, 187-197 Application of Thallium Isotopes: Tracking Marine Oxygenation through Manganese Oxide Burial.	o 5-5	1 1 30 32 13
76 75 74 73 72	Encyclopedia of Geochemistry. Encyclopedia of Earth Sciences Series, 2016, 1-4 Encyclopedia of Geochemistry. Encyclopedia of Earth Sciences Series, 2018, 947-950 Uranium isotopes in marine carbonates as a global ocean paleoredox proxy: A critical review. Geochimica Et Cosmochimica Acta, 2020, 287, 27-49 Delayed Neoproterozoic oceanic oxygenation: Evidence from Mo isotopes of the Cryogenian Datangpo Formation. Precambrian Research, 2018, 319, 187-197 Application of Thallium Isotopes: Tracking Marine Oxygenation through Manganese Oxide Burial. 2019, Bistability in the redox chemistry of sediments and oceans. Proceedings of the National Academy of	5.5	1 1 30 32 13

68	Contrasting nutrient availability between marine and brackish waters in the late Mesoproterozoic: Evidence from the ParanolGroup, Brazil. <i>Geobiology</i> , 2021 ,	4.3	1
67	High authigenic Co enrichment in the non-euxinic buff-grey and black shale of the Chandarpur Group, Chhattisgarh Supergroup: Implication for the late Mesoproterozoic shallow marine redox condition. <i>Terra Nova</i> , 2022 , 34, 72	3	
66	Fossil evidence provides new insights into the origin of the Mesoproterozoic ministromatolites. <i>Precambrian Research</i> , 2021 , 366, 106426	3.9	
65	Encyclopedia of Geochemistry. Encyclopedia of Earth Sciences Series, 2017, 1-6	Ο	
64	Encyclopedia of Geochemistry. Encyclopedia of Earth Sciences Series, 2018, 751-756	О	
63	Insights into the evolution of oxygenic photosynthesis from a phylogenetically novel, low-light cyanobacterium.		O
62	Defining the toxicity limits on microbial range in a metal-contaminated aquifer Running Title: Inorganic ion toxicity limits on microbial range.		
61	Encyclopedia of Astrobiology. 2020 , 1-5		
60	The Mesoproterozoic Oxygenation Event. Science China Earth Sciences, 2021, 64, 2043	4.6	4
59	Significance of Trace Elements in Marine Shale Pyrite for Reconstructing the Sedimentary Environment: A Case Study of Niutitang and Hongshuizhuang Formations. <i>ACS Earth and Space Chemistry</i> ,	3.2	O
58	Tectonic controls on sedimentary provenance and basin geography of the Mesoproterozoic Wilton package, McArthur Basin, northern Australia. <i>Geological Magazine</i> , 1-20	2	2
57	Inverse methods for consistent quantification of seafloor anoxia using uranium isotope data from marine sediments. <i>Earth and Planetary Science Letters</i> , 2022 , 577, 117240	5.3	3
56	Application of Cd as a paleo-environment indicator. <i>Palaeogeography, Palaeoclimatology, Palaeoecology</i> , 2021 , 110749	2.9	O
55	Quantifying the Seawater Sulfate Concentration in the Cambrian Ocean. <i>Frontiers in Earth Science</i> , 2021 , 9,	3.5	1
54	B3Cr values of catchment runoff exhibit seasonality regardless of bedrock Cr concentrations: Role of periodically changing chromium export fluxes. <i>Hydrological Processes</i> , e14434	3.3	1
53	Atmospheric oxygen abundance, marine nutrient availability, and organic carbon fluxes to the seafloor. Global Biogeochemical Cycles,	5.9	O
52	Using whole rock and in situ pyrite chemistry to evaluate authigenic and hydrothermal controls on trace element variability in a Zn mineralized Proterozoic subbasin. <i>Geochimica Et Cosmochimica Acta</i> , 2022, 318, 366-387	5.5	O
51	Geochemical Records Reveal Protracted and Differential Marine Redox Change Associated With Late Ordovician Climate and Mass Extinctions. <i>AGU Advances</i> , 2022 , 3,	5.4	3

Chimeric Inheritance and Crown-Group Acquisitions of Carbon Fixation Genes within Chlorobiales.

49	Peptides before and during the nucleotide world: an origins story emphasizing cooperation between proteins and nucleic acids <i>Journal of the Royal Society Interface</i> , 2022 , 19, 20210641	4.1	6
48	Marine Cyanobacteria. The Microbiomes of Humans, Animals, Plants, and the Environment, 2022, 103-157		
47	“????”???????“??????”. <i>Chinese Science Bulletin</i> , 2022 ,	2.9	O
46	Molybdenum isotope-based redox deviation driven by continental margin euxinia during the early Cambrian. <i>Geochimica Et Cosmochimica Acta</i> , 2022 ,	5.5	2
45	Palaeoenvironments and elemental geochemistry across the Permian-Triassic boundary at Ursula Creek, British Columbia, Canada, and a comparison with some other deep-water Permian-Triassic boundary shelf/slope sections in western North America. <i>Depositional Record</i> ,	2	
44	Chromium isotope evidence for oxygenation events in the Ediacaran ocean. <i>Geochimica Et Cosmochimica Acta</i> , 2022 , 323, 258-275	5.5	0
43	Chromium evidence for protracted oxygenation during the Paleoproterozoic. <i>Earth and Planetary Science Letters</i> , 2022 , 584, 117501	5.3	O
42	Mineral paragenesis in Paleozoic manganese ore deposits: Depositional versus post-depositional formation processes. <i>Geochimica Et Cosmochimica Acta</i> , 2022 , 325, 65-86	5.5	0
41	Binding and transport of Cr(III) by clay minerals during the Great Oxidation Event. <i>Earth and Planetary Science Letters</i> , 2022 , 584, 117503	5.3	O
40	A potential linkage between excess silicate-bound nitrogen and N2-rich natural gas in sedimentary reservoirs. <i>Chemical Geology</i> , 2022 , 600, 120864	4.2	
39	Image_1.pdf. 2019 ,		
38	Table_1.xlsx. 2019 ,		
37	Table_2.xlsx. 2019 ,		
36	Characterization of diverse bacteriohopanepolyols in a permanently stratified, hyper-euxinic lake. <i>Organic Geochemistry</i> , 2022 , 104431	3.1	
35	Chromium isotope fractionation during magmatic processes: Evidence from mid-ocean ridge basalts. <i>Geochimica Et Cosmochimica Acta</i> , 2022 , 327, 79-95	5.5	O
34	Constraining the redox landscape of Mesoproterozoic mat grounds: A possible oxygen oasis in the B oring Billion eafloor. <i>Precambrian Research</i> , 2022 , 376, 106681	3.9	1
33	Characteristics of the carbon cycle in late Mesoproterozoic: Evidence from carbon isotope composition of paired carbonate and organic matter of the Shennongjia Group in South China. <i>Precambrian Research</i> , 2022 , 377, 106726	3.9	O

32	Mo isotope composition of the 0.85 Ga ocean from coupled carbonate and shale archives: Some implications for pre-Cryogenian oxygenation. <i>Precambrian Research</i> , 2022 , 378, 106760	
31	Geoelectric constraints on the Precambrian assembly and architecture of southern Laurentia. 2022,	1
30	The evolution and spread of sulfur-cycling enzymes reflect volcanic sulfur sources and the redox state of the early Earth.	
29	Low oxygen seawater and major shifts in the paleoenvironment towards the terminal Ediacaran: Insights from the Portfjeld Formation, North Greenland. 2022 , 379, 106781	Ο
28	Mechanisms of chromium isotope fractionation and the applications in the environment. 2022 , 242, 113948	
27	Formation of the massive bedded chert and coupled Silicon and Iron cycles during the Ediacaran-Cambrian transition. 2022 , 594, 117721	
26	Impact of estuaries on fluvial Cr input into the ocean: Perspectives from the Mobile Bay Estuary, Northern Gulf of Mexico. 2022 , 334, 187-200	
25	What besides redox conditions? Impact of sea-level fluctuations on redox-sensitive trace-element enrichment patterns in marine sediments. 2022 , 65, 1985-2004	O
24	???????????????——?????. 2022 ,	O
23	Chromium cycling in redox-stratified basins challenges Б 3 Cr paleoredox proxy applications.	Ο
22	A stable and moderate nitrate pool in largely anoxic Mesoproterozoic oceans and implications for eukaryote evolution. 2022 , 381, 106868	0
21	Nitrogen Isotopes from the Neoproterozoic Liulaobei Formation, North China: Implications for Nitrogen Cycling and Eukaryotic Evolution. 2022 , 33, 1309-1319	Ο
20	Chimeric inheritance and crown-group acquisitions of carbon fixation genes within Chlorobiales: Origins of autotrophy in Chlorobiales and implication for geological biomarkers. 2022 , 17, e0275539	0
19	Extant mat microbes synchronize vertical migration to a diel tempo. 2022,	Ο
18	Microfabrics and organominerals as indicator of microbial dolomite in deep time: An example from the Mesoproterozoic of North China. 2022 , 382, 106881	0
17	No evidence for expansion of global ocean euxinia during the base Stairsian mass extinction event (Tremadocian, Early Ordovician). 2023 , 341, 116-131	Ο
16	Vanadium isotope evidence for widespread marine oxygenation from the late Ediacaran to early Cambrian. 2023 , 602, 117942	0
15	Early diagenetic processes in an iron-dominated marine depositional system. 2023 , 341, 183-199	O

14	Evaluation of the molybdenum isotope system as a petroleum tracer: The Phosphoria petroleum system, western U.S.A 2023 , 617, 121244	O
13	Chromium stable isotope distributions in the southwest Pacific Ocean and constraints on hydrothermal input from the Kermadec Arc. 2023 , 342, 31-44	O
12	Reduced Marine Molybdenum Inventory Related to Enhanced Organic Carbon Burial and an Expansion of Reducing Environments in the Toarcian (Early Jurassic) Oceans. 2022 , 3,	O
11	Protracted oxygenation across the Cambrian Drdovician transition: A key initiator of the Great Ordovician Biodiversification Event?.	O
10	Geochemical conditions regulating chromium preservation in marine sediments. 2023, 348, 239-257	O
9	Coupled vanadium and thallium isotope constraints on Mesoproterozoic ocean oxygenation around 1.38-1.39 Ga. 2023 , 610, 118127	O
8	Microbe-mediated, marine authigenic formation of ooidal chamosite: Insights from upper Ordovician carbonates of the South-Western Yangtze platform (China).	O
7	Global ocean redox changes before and during the Toarcian Oceanic Anoxic Event. 2023, 14,	O
6	Basin-scale reconstruction of euxinia and Late Devonian mass extinctions. 2023, 615, 640-645	O
5	Redox-sensitive elements of Ediacaran black shales in South China with implications for a widespread anoxic ocean. 2023 , 251, 105670	O
4	Origin of Banded Iron Formations: Links with Paleoclimate, Paleoenvironment, and Major Geological Processes. 2023 , 13, 547	О
3	Viruses of sulfur oxidizing phototrophs encode genes for pigment, carbon, and sulfur metabolisms. 2023 , 4,	O
2	Evolutionary stasis during the Mesoproterozoic Columbia-Rodinia supercontinent transition. 2023 , 391, 107057	O
1	Widespread seafloor anoxia during generation of the Ediacaran Shuram carbon isotope excursion.	O